Energy Storage and Conversion 2026, 4(1), 4043.
doi: https://doi.org/10.59400/esc4043

Article

Thermodynamic investigation of a diffusion absorption refrigeration system with an isobutane–dimethylformamide–helium working fluid blend

Sreenesh Valiyandi*, Gireeshkumaran Thampi

Division of Mechanical Engineering, School of Engineering, Cochin University of Science and Technology, Ernakulam 682022, India
*** Corresponding author:** Sreenesh Valiyandi, sreenesh8569@gmail.com

CITATION

Valiyandi S, Thampi G. Thermodynamic investigation of a diffusion absorption refrigeration system with an isobutane–dimethylformamide–helium working fluid blend. Energy Storage and Conversion. 2026; 4(1): 4043. https://doi.org/10.59400/esc4043

ARTICLE INFO

Received: 1 February 2026
Revised: 7 March 2026
Accepted: 11 March 2026
Available online: 12 March 2026

Abstract: Diffusion absorption refrigeration (DAR) is a promising cycle concerning renewable energy utilization, as the cycle can operate using only thermal energy input. However, to realize the benefits of the DAR cycle, there is a need to develop an improved understanding of how design parameters influence its performance. The cycle's performance was particularly sensitive to several factors: the rate of heat added and the temperature of the generator, the effectiveness of the gas and solution heat exchangers, the mass flow rate of the refrigerant, and the type of working fluid. The aim of this research work is to conduct numerical simulations of the diffusion absorption refrigeration (DAR) cycle to study the thermodynamic performances. The working fluids utilized in this system are isobutane (R600a) (C4H10) as a refrigerant, dimethylformamide $(CH_3)_2NC(O)H$, as absorbent and helium as the inert gas. The cycle operation characteristics are investigated through numerical analysis, in terms of the coefficient of performance (COP) and minimum temperature by using the effect of generator temperature, absorber temperature, evaporator temperature and the solution concentrations. The performance of the system is examined by computer simulation using MATLAB software. The mathematical model will provide a reasonable estimation of the maximum COP, cooling capacity, mass flow rate, and exergy analysis. The refrigeration cycle experiments were conducted under the ambient condition of 30 °C. Based on a mathematical model, performance evaluation and exergy analysis of the system are performed. The experiment set included a 0.04 m^3 volume of commercial absorption diffusion refrigerator working with the dimethylformamide $(CH_3)_2NC(O)H$ solution. Furthermore, the results obtained in the proposed system compare with the previous studies.

Keywords: diffusion absorption refrigeration; isobutane; dimethylformamide; helium; coefficient of performance; cooling capacity; mass flow rate; exergy analysis

1. Introduction

In the last decades, there has been an inevitable increase in the demand for refrigeration and air-conditioning devices to fulfil basic and comfort needs in different sectors of society [1]. Refrigeration technology based on vapour compression is the leading technology in the world, which is an indirect cause of greenhouse gas emissions due to the type of energy it uses. Accordingly, it consumes nearly 30% of the final energy in the world [2]. Furthermore, developing countries continue to use compression systems based on refrigerant fluids that damage the ozone layer, and represent a high global warming potential (GWP) [3]. New technologies have emerged in response to the search for better alternatives that would not have damaging effects on the

environment. These technologies are characterized by the type of activation energy, such as the use of renewable energy, including solar, geothermal, residual heat, etc., which can be translated to a reduction of greenhouse gas emissions, and the working fluids that they use do not contribute to global warming [4]. Among these technologies, refrigeration systems by absorption are the most commonly used for refrigeration and air conditioning applications, which have been demonstrated to have the same cooling capacity, the total energy consumed and the total cost is less than a vapour compression system [5].

Diffusion absorption cycles (DARs) for refrigeration or air-conditioning systems have recently attracted great attention. Due to 7% of global energy consumption is related to cooling processes [6]. Moreover, while some researchers are expected to double their space cooling capacity by 2030, Asian countries' demand for energy makes them the dominant energy consumers in cooling [7]. About this increasing demand, conventional refrigeration systems (vapour-compression refrigeration systems) are being developed to operate with renewable energy inputs as hybrid cooling systems [8]. However, hybrid systems can be harmful to the environment due to the depletion of the ozone layer and the effects of greenhouse emissions. Consequently, DAR systems have some important advantages that reduce greenhouse emissions and other harmful effects on the environment. DAR can be defined as one of the absorption cycles, which is quite useful with its distinct advantages, especially in small-scale applications [9]. Subsequently, it only refers to a single pressure cycle in which the circulation of the working fluid can provide a bubble pump (thermally driven), so no electrical input is required for circulating the working fluid. Generally, the DAR systems are commonly used in recreational vehicles, campers, hotels, and caravans because they can be powered with propane fuel, rather than electricity. In addition to this advantage, low noise levels, and low construction and maintenance costs are other advantages of the DAR system [10]. However, a typical low-performance problem exists with the DAR systems.

In DAR, the activation of the system is provided by renewable energy sources, such as solar, geothermal and waste heat, as well as electricity. Additionally, this technology is becoming a new trend and a developing field in the literature [11]. Moreover, the absence of moving parts in DAR provides the advantage of quiet operation, comparable to other mechanical systems, as well as the need for less maintenance. Subsequently, there are many studies in the literature that have investigated DARs. The DAR system unit's thermal performance was assessed for its efficiency. Key benefits of the system include its ability to resist crystallization and corrosion, while heat transfer at varying temperatures contributes significantly to exergy loss in the DARS system [12]. Chen carried out a study by manufacturing a new boiler with a heat exchanger in a DAR. They indicated that the COP of the system was 0.3, which led to an increase of more than 50% of the COP. In a similar study, Gurevich and Zohar [13] created three different designs for the boiler and bubble pump. Accordingly, they first developed the boiler and the bubble pump in a nested structure (normal structure), and in the second and third designs the boiler and the bubble pump were completely separated and partially separated. Most of

them focused on the determination of its favorable operation temperatures, improving the cycle performance, using different heat sources and examining different working fluid pairs [14]. The selection of an appropriate working fluid pair can significantly influence the performance, the capital cost and the maintenance period of the absorption refrigeration system. In the absorption refrigeration market, some systems use the H_2O-LiBr pair and the NH_3-H_2O pair for air-conditioning and refrigeration [15]. To overcome the low coefficient of performance (COP) barrier, new techniques, and new materials need to work in several roles. Furthermore, low-cost methods have been developed to increase the thermal conductivity of the coolant.

The performance of a DAR system using organic working fluids with DMAC as absorbent and helium as a non-reacting component is analyzed and compared with an ammonia-water-hydrogen system. The NH_3-H_2O-He blend exhibits the highest COP of 0.298 at a low circulation ratio compared to the organic working fluids [16].

Adjibade et al. [17] studied the performance of the DAR system using ammonia-water-hydrogen working fluid and reported COP of 0.298. Similarly, Elsayed et al. [18] investigated ammonia/water and hydrogen-based DAR systems, optimizing cycle configurations through Aspen HYSYS. Sreenesh Valiyandi and Gireeshkumaran Thampi [19] studied the performance of a diffusion absorption refrigeration system with different working fluids. The results show that an optimized blend of isobutane, dimethylformamide, and helium exhibits maximum performance. Gawon Lee et al. [20] presented an experimental investigation of a DAR system using the working fluid R600a/n-octane and compared it with simulation results. The operation parameters were determined through numerical methods, regarding the minimum temperature and the coefficient of performance. The experimental COP values are close to the simulation results, and the maximum COP exhibited was 0.162 at a driving temperature of 100 ℃. R600a/n-octane shows higher performance than other low GWP refrigerant combinations used for solar cooling.

Adnan Sözen et al. [21] experimentally examined the influence of passive heat transfer improvement with different nanofluids consisting of magnesium oxide aluminate spinel (MgO-Al_2O_3) at different rates. A DAR system using nanofluid performs rapid evaporation, reduces operation time, and augments heat transfer in the generator. In addition, 2% nanofluid in a DAR system shows a 37.4% improvement in COP and a 44.2% uplift in exergetic performance compared to a DAR system lacking nanoparticles.

Senthilkumar et al. [22] investigated the performance of a vapour compression refrigeration system using R600a refrigerant with hybrid nano lubricants (CuO/Al_2O_3). The experiment was performed to examine power consumption, COP, cooling effect, transmittance, and pulldown of a refrigerator with nano doped mineral oil and hybrid nanoparticles with lubricants, compared to mineral oil without nanoparticles. The incorporation of CuO/Al_2O_3 into lubricating oil improved performance by 27% (from 1.17 to 1.6), enhanced cooling capacity by 20% (from 160 to 200 W), and minimized power consumption of the compressor by 24% (from 158 W to 120 W) compared to without nanofluids.

Cuma Çetiner [23] studied the electric and solar-powered diffusion-absorption

refrigerators, finding the electric version performed better with a COP of 0.398 and an evaporator temperature of −10 ℃. The solar refrigerator had a COP of 0.38 and evaporator temperature of 1 ℃, hindered by variable solar energy and collector inefficiencies. A phase change material and battery bank are proposed to improve solar refrigerator performance in low-sunlight conditions.

R. Garma et al. [24] conducted an experimental diffusion-absorption refrigerator using low-GWP n-butane, n-nonane, and helium and showing a maximum COP of 0.175 at 260 W heating power with a cooling capacity of 58 W. The system's performance decreased with increased cooling medium temperature, requiring higher generator temperatures. A validated HYSYS simulation model predicted a COP drop from 0.23 to 0.125 when the cooling air temperature rose from 27 ℃ to 35 ℃

Sreenesh Valiyandi and Gireeshkumaran Thampi [25] examined the performance of the DAR system with five different working fluid blends and studied the effect of rich solution concentration on performance matrices. The outcome of this research reveals that the isobutane–dimethylformamide–helium blend in a DAR system shows maximum performance at minimum concentration compared to other blends.

Asmaa A. Harraz et al. [26], introduce a unified framework for computer-aided molecular and diffusion absorption refrigeration (CAMD-DAR) system design, which integrates a group-contribution equation-of-state based on the statistical associating fluid theory (SAFT-γ Mie) for simultaneous working-fluid design and property prediction, alongside DAR module design. The findings indicate that combining non-polar organic refrigerants with polar absorbents is the best approach to achieve maximum cooling rates in a conventional DAR module design, with a specific mixture of 2-butene (2-C_4H_8) and ethanol (C_2H_5OH) pressurized by helium emerging as the optimal working fluid for diverse cooling and ambient temperature applications.

Gurevich [27] examines the impact of magnesium aluminate spinel nanoparticles on a low-pressure, low-GWP diffusion-absorption refrigerator's performance. The nanoparticles improved start-up time and increased the generator's heat duty and overall heat-transfer coefficient, with optimal performance at 0.0021–0.0042 wt% loading. An exergy analysis assessed the second-law performance, providing insights into the nanoparticles' effectiveness.

S. Zebbar et al. [28] present a CFD simulation of a DAR evaporator using a water-ammonia mixture with helium as a safer alternative to hydrogen. The study investigates evaporator behavior at 10–25 bar pressures to determine optimal pressure with helium, building on a validated CONVERGE CFD model. The outcomes unveil that the least total pressures (10–12 bar) improve evaporation and heat transfer in a water-ammonia DAR system with helium, maximizing cooling capacity. Helium enhances safety and efficiency, making it a viable alternative to hydrogen, especially for solar-driven systems.

Several works have been done in DAR systems using conventional working fluids, ammonia–water–hydrogen or helium combination, but the limited studies were carried out with organic working fluids like isobutane–dimethylformamide–helium blend. The research concentrates on the performance analysis of the DAR system functioned by R600a–DMF–He blend.

The paper underscores the relevance of working fluid, refrigerant mass flow rate, heat exchanger efficiency, and generator temperature in determining system performance. The work emphasizes the possibility of advanced simulation for optimizing renewable energy-based refrigeration systems. The research aims at the thermodynamic analysis of DAR systems using isobutane (C_4H_{10}) as a refrigerant, dimethylformamide (DMF) as an absorbent and inert gas used is helium.

This research work is structured as follows: Section 1 presents the introduction, which consists of a literature review and motivation. Section 2 demonstrates the system description and working fluids used in DAR system follow the mathematical modelling, including numerical simulation procedure and experimental validation in Section 3. Section 4 illustrates the result and discussion and follows the conclusion and future recommendations in Section 5.

2. System description and working fluids

This study looks at how well a diffusion absorption refrigeration (DAR) system works, using both computer simulations and real-world tests. The system uses isobutane (C_4H_{10}) as the refrigerant, dimethylformamide (DMF) as the absorbent, and helium as the inert gas. This working fluid blend was chosen because of its good thermodynamic properties, minimal environmental effects, and applicability for low-grade heat-driven refrigeration systems. Helium is used in DAR systems as a non-reactive component to equalize the pressure and increase mass diffusion within the cycle. **Figure 1** shows the schematic diagram of the DAR system. Here's how it runs: Heat goes into the generator and warms up the strong solution, which turns the refrigerant into vapor. A bubble pump lifts that vapor up to the rectifier, which strips out any leftover absorbent. Then the purified refrigerant moves to the condenser, cools down, and turns back into a liquid. After that, the liquid refrigerant heads to the evaporator. There, it picks up heat and evaporates—helium's present too—creating the cooling effect. The vaporized refrigerant goes to the absorber, where the dimethylformamide soaks it up. That solution goes back to the generator, and the whole process repeats.

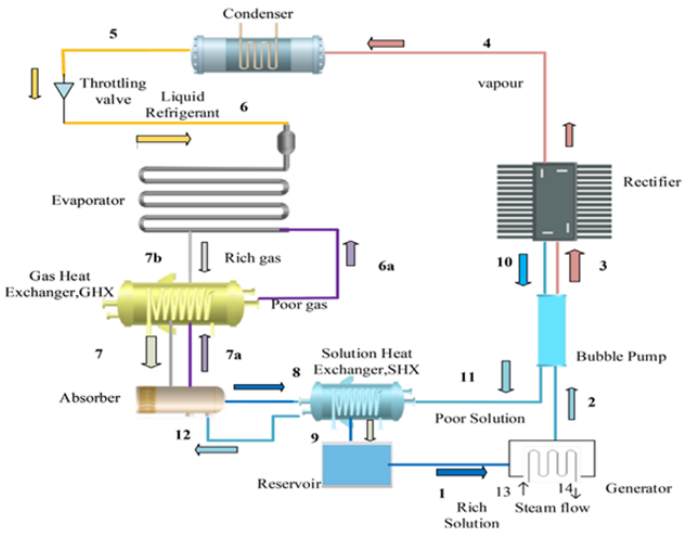

Figure 1. Diffusion absorption refrigeration system.

3. Mathematical modeling of the DAR cycle

A mathematical model of the DAR system was created to depict the thermodynamic behavior of individual system components, comprising the evaporator, absorber, solution heat exchanger, condenser, generator and rectifier. The model is developed on the basic conservation equations of mass, energy, and exergy, assuming one-dimensional flow and thermodynamic equilibrium at each state point. Pressure drops in the components were neglected and heat losses to the surroundings were considered as needed to simplify the analysis. **Table 1** shows the mass and energy balance equations of DAR system.

Table 1. Mass and energy balance equations.

Components	Mass balance	Energy balance
Evaporator	$\dot{m}_{7b} = \dot{m}_{6a} + \dot{m}_6$	$\dot{m}_{6a}h_{6a} + \dot{m}_6h_6 = Q_{evap} + \dot{m}_{7a}h_{7a}$
Absorber	$\dot{m}_{7b} = \dot{m}_{6a} + \dot{m}_6$	$\dot{m}_7h_7 + \dot{m}_{12}h_{12} = Q_{ab} + \dot{m}_8h_8$
Generator	$\dot{m}_1 + \dot{m}_{13} = \dot{m}_2 + \dot{m}_{14}$	$\dot{m}_1h_1 + Q_g = \dot{m}_2h_2 + \dot{m}_{14}h_{14}$
Bubble pump	$\dot{m}_2 + \dot{m}_{10} = \dot{m}_3 + \dot{m}_{11}$	$\dot{m}_2h_2 + \dot{m}_{10}h_{10} = \dot{m}_3h_3 + \dot{m}_{11}h_{11}$
Condenser	$\dot{m}_4 = \dot{m}_5$	$Q_{cond} = \dot{m}_4h_4 - \dot{m}_5h_5$
Gas Heat Exchanger (GHX)	$\dot{m}_{7a} + \dot{m}_{7b} = \dot{m}_7 + \dot{m}_6$	$\dot{m}_{7a}h_{7a} + \dot{m}_{7b}h_{7b} = \dot{m}_7h_7 + \dot{m}_6h_6$
Solution Heat Exchanger (SHX)	$\dot{m}_8 + \dot{m}_{11} = \dot{m}_9 + \dot{m}_{12}$	$\dot{m}_8h_8 + \dot{m}_{11}h_{11} = \dot{m}_9h_9 + \dot{m}_{12}h_{12}$
Rectifier	$\dot{m}_3 = \dot{m}_4 + \dot{m}_{10}$	$\dot{m}_4h_4 + \dot{m}_{10}h_{10} = Q_{rect} + \dot{m}_3h_3$

Thermophysical properties of the working fluids, comprising viscosity, density, specific heat, and thermal conductivity, were attained from reliable thermodynamic databases and literature sources. The model estimates crucial performance parameters such as refrigerant mass flow rate, cooling capacity, coefficient of performance (COP), and exergy efficiency.

3.1. Numerical simulation procedure

Numerical simulations were executed using MATLAB software to determine system performance. System parameters including evaporator temperature, generator temperature, absorber temperature, and solution concentration were varied systematically to evaluate their influence on cooling capacity and COP. The model was solved iteratively until convergence was reached for all governing equations. Special attention was given to optimizing the concentration and operating temperatures to improve system stability and performance during dynamic operation.

3.2. Experimental validation

Experimental analysis were conducted using a commercial diffusion absorption refrigeration system with a total volume of 0.04 m^3 and validated with a numerical model. The experiments were conducted under a controlled atmospheric temperature of 30 ℃. Thermal indicators are placed at key locations to measure temperatures of the components comprising the condenser, generator, absorber, and evaporator. **Figure 2** displays the experimental setup of the DAR system.

The performance of the system is estimated by multiple metrics, comprising refrigeration effect, cooling capacity, optimum COP, and exergy efficiency. These

parameters are analyzed to evaluate the optimal operating conditions and to examine the effectiveness of the proposed working fluid blend. The methodology delivers a vigorous framework for optimizing DAR system performance and sustains the advancement of efficient, renewable energy-driven refrigeration technologies.

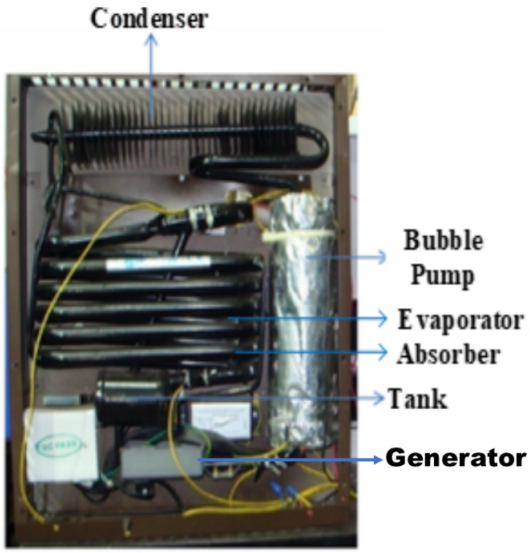

Figure 2. Experimental setup.

4. Results and discussion

4.1. Effect of driving temperature on COP at different operating pressures

Figure 3 presents the effect of the coefficient of performance (COP) on driving temperature at various system pressure ranges from 400 to 600 kPa. At the early stages COP augments with driving temperature, attains an optimum at a particular temperature, and then decreases as temperature increases.

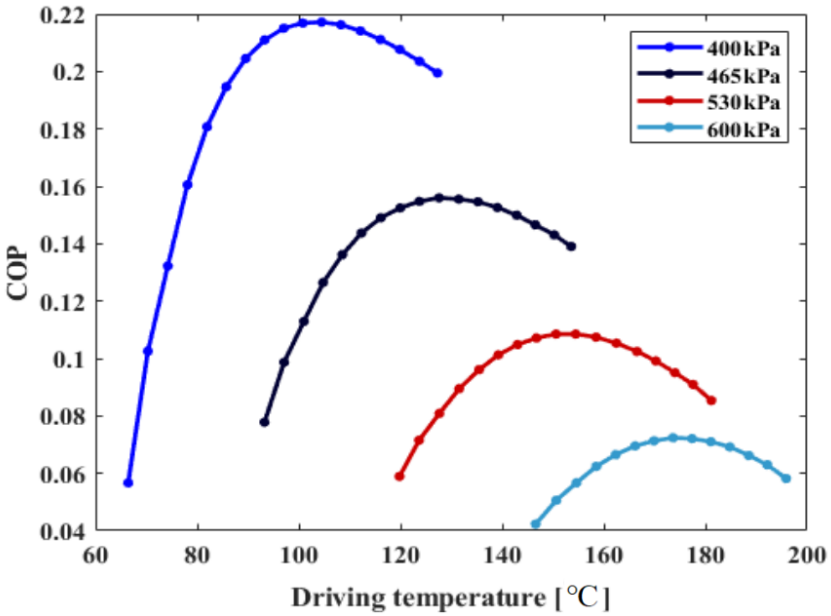

Figure 3. COP variation with different total pressures.

This trend represents the existence of an optimal driving temperature at

equilibrium between refrigerant circulation and heat input is attained. Larger values of COP are exhibited at lower pressures (400 and 465 kPa), and the optimum COP of 0.22 at the driving temperature of 90–100 °C for the driving pressure of 400 kPa. At the pressures of 530 and 600 kPa the maximum COP reduces notably and changes towards larger driving temperatures. This performance reduction at higher pressures is due to the enhancement of the circulation ratio, irreversibilities and decreased mass and heat transfer effectiveness during the process. The outcome clearly presents that minimum operating pressures combined with moderate driving temperature uplift the performance of DAR system. These results emphasize the significance of optimizing pressure of the system and driving temperature to attain advancement of performance, especially for low-grade heat applications.

4.2. Effect of driving temperature on strong solution concentration on various operating pressures

The effect of solution concentration (Xs) on driving temperature at various operating pressures ranging from 400 to 600 kPa is exhibited in **Figure 4**. The solution concentration shows a reducing behavior with the rising driving temperature. This trend is attributed to increased refrigerant desorption from the absorbent at larger generator temperatures, which minimizes the mass fraction of the refrigerant in the solution.

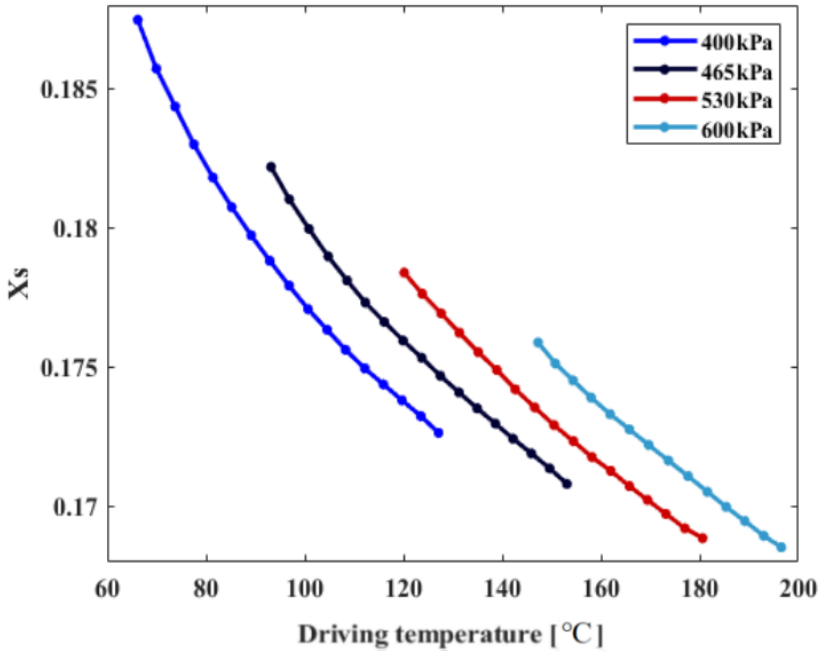

Figure 4. Total pressure on strong concentration solution.

The increased solution concentration is seen at least operating pressures (400 and 465 kPa) for the entire temperature span, showing highly effective circulation of the refrigerant and greater absorption capability within the cycle. The strong solution concentration reduces significantly and shifts towards. More driving temperatures at the rising operating pressures range from 530 to 600 kPa. The lowering of strong solution concentration at elevated pressures is due to decreased solubility of the refrigerant in the absorbent and larger generator thermal loads. The outcomes reveal

that maintaining smaller operating pressure and moderate driving temperature prefer the stronger solution concentrations, which is necessary for attaining stable cycle operation, enhanced mass transfer and increased overall performance of the diffusion absorption refrigeration system.

4.3. Effect of mass flow rate on driving temperature at different operating pressures

The effect of mass flow rate on driving temperature at various operating pressures (400, 465, 530 and 600 kPa) is displayed in **Figure 5**. The mass flow rate consistently reduces at all pressure levels as the driving temperature rises, showing strong inverse relationship with these two parameters. At minimum driving temperature (70–100 ℃) higher mass flow rates are noted with values attaining up to 0.11 kg s^{-1} at 400 kPa. As the driving temperature increases, the mass flow rate continuously reduces, dropping below 0.05 kg s^{-1} at temperatures more than 160 ℃ for higher pressure conditions. This trend can result in the associated variations in thermodynamic properties of the working fluid at moderate temperatures and a decrease in density which restricts the effective circulation in the system. The higher operating pressures tend to maintain comparatively higher mass flow rates specifically at moderate temperatures. For example, driving temperature more than 140 ℃, the 600 kPa shows significantly increased mass flow rate compared to lower operating pressures. This implies that augmenting system pressure partially shifts the detrimental effect of higher driving temperatures by improving driving potential for circulation of the working fluid.

Overall, the outcomes unveil that while increasing the driving temperature, decreases the mass flow rate at all pressures, operating at higher pressures can mitigate this reduction to some extent. These results are crucial for optimizing system performance, as they represent an appropriate combination of operating pressure and driving temperature that is vital to ensure stable operation and sufficient mass flow rate.

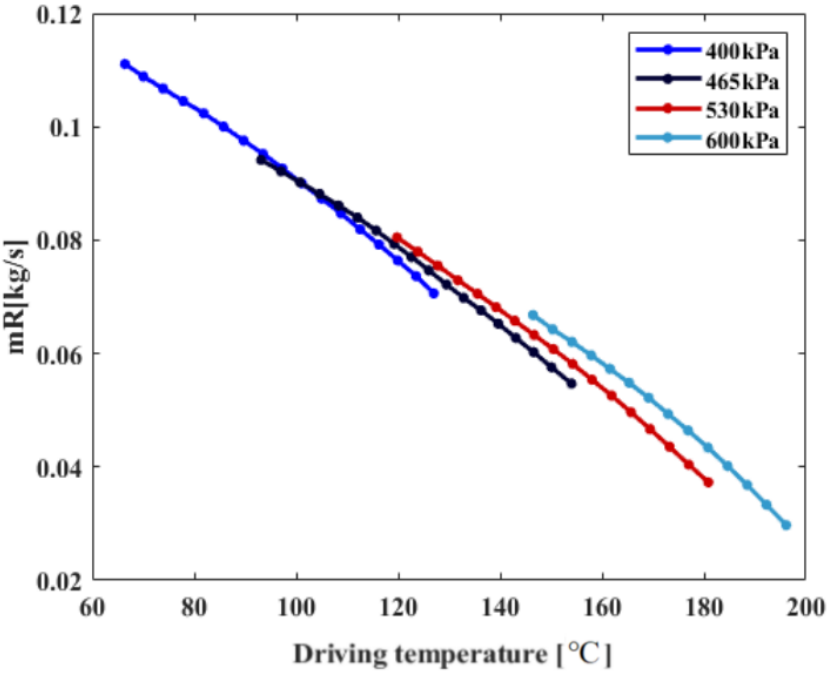

Figure 5. Mass flow rate with driving temperature.

4.4. Effect of circulation ratio on driving temperature at various operating pressures

The circulation ratio (f) is the ratio of the flow rate of the rich solution to the flow rate of refrigerant vapor generated in the bubble pump. The performance graph for the circulation ratio on driving temperature at different operating pressures (400, 465, 530 and 600 kPa) is portrayed in **Figure 6**. The circulation ratio increases with increasing driving temperature. When the driving temperature is 60 to 130 ℃, the circulation ratio is between 7 and 14 for 400 kPa. Accordingly, the circulation ratio is 10 to 14.5 when the driving temperature is 90 to 160 ℃ for 465 kPa. Subsequently, the circulation ratio reaches 11 to 15.6 for 530 kPa during the 120 ℃ to 180 ℃. Additionally, when the temperature is 145 ℃ to 197 ℃, then the circulation ratio is 12.9 to 15.9 for 600 kPa, respectively. The lower value of circulation ratio is obtained at an operating pressure of at least 400 kPa. The f increases steeply at lower driving temperatures followed by a steady increase at higher temperatures. This behavior recommends that the enhancement of solution circulation and vapor generation becomes less noticeable at moderate temperatures due to thermodynamic and transport limitations within the system.

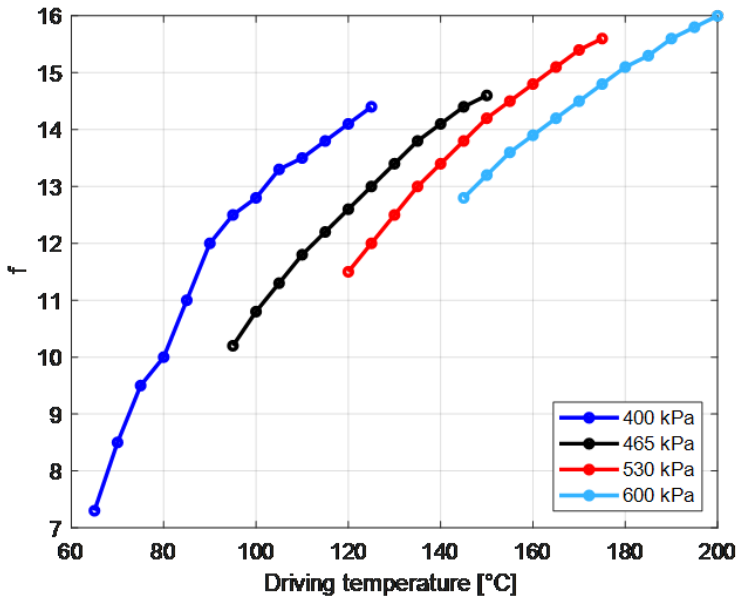

Figure 6. Circulation ratio during the driving temperature.

Overall, the results indicate that increasing the driving temperature and operating pressure both contribute to enhanced circulation ratio. These results are vital for the optimal design and operation of the system, as they underscore the need to balance pressure and driving temperature to maximize circulation performance without unnecessary thermal input.

4.5. Influence of driving temperature on weak solution concentration at different operating pressures

The performance graph of weak solution concentration (X_w) on driving temperature at various operating pressures (400, 465, 530 and 600 kPa) is exhibited

in **Figure 7**. A steady diminishing trend of (X_w) at increasing driving temperature is seen at all operating pressures, representing a significant inverse relationship between thermal input and weak solution concentration. Higher weak solution concentration of 0.10 is observed at lower driving temperature during minimum operating pressure of 400 kPa. The weak solution drops below 0.03 when the driving temperature increases above 150 ℃ in a majority of operating conditions. The decreasing behavior of weak solution is due to improved vapor generation at higher generator temperatures which tends to increase separation of the refrigerant from the solution and additionally it lowers the mass fraction.

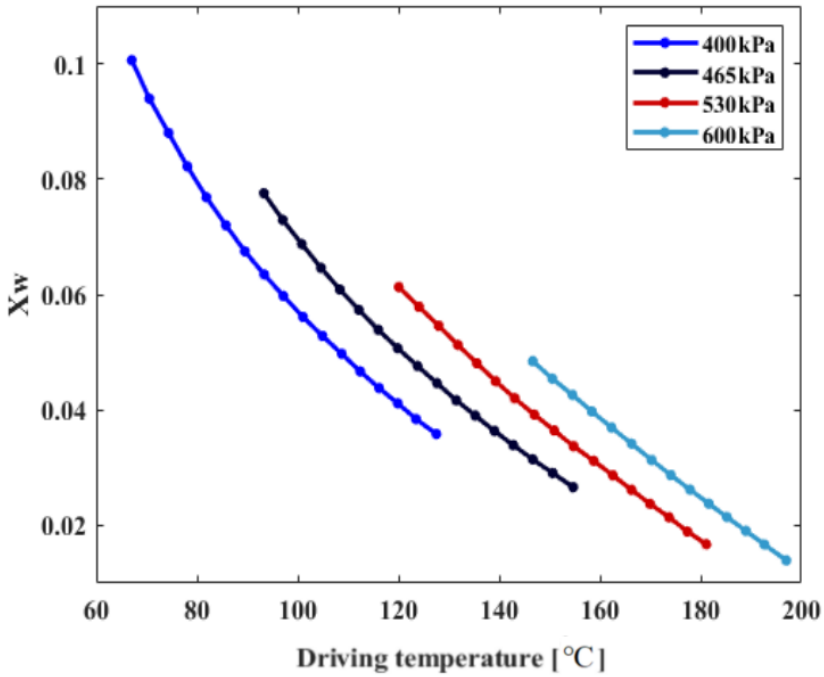

Figure 7. Variation of driving temperature on the concentration of weak solution at different operating pressures.

Operating pressure has a significant effect on the value of X_w. For a given driving temperature, higher pressures correspond to lower weak solution concentration. For instance, at approximately 140 ℃, X_w decreases from 0.035 at 465 kPa to nearly 0.028 at 530 kPa, and further to about 0.025 at 600 kPa. This trend is evident that moderate pressures increase the desorption process, promoting stronger refrigerant separation and yielding a more dilute weak solution.

In addition, the curves show a steeper fall at reduced driving temperatures, followed by a greater steady reduction at higher temperatures. This shows that the sensitivity of weak solution concentration to temperature is more evident in the low-to-moderate temperature range, while at higher temperatures the system approaches a regime where further thermal input produces diminishing changes in solution composition.

Overall, the results illustrate that increasing operating pressure and driving temperature both result in a reduction in weak solution mass fraction, which shows an improved generator performance. In addition, excessive reductions in X_w may also influence system control and solution circulation stability. Therefore, an optimal

balance between pressure and driving temperature is necessary to ensure efficient refrigerant separation while maintaining stable system operation.

4.6. Effect of COP on driving temperature at varying heat exchanger effectiveness and minimum temperature

The way driving temperature influences the coefficient of performance at the minimum temperature depending on the effectiveness of the solution heat exchanger (ε_{SHX}) 0.80, 0.85 and 0.90 is shown in **Figure 8**. The COP goes up as the driving temperature rises, reaching its highest point before it starts to drop when the temperature gets even higher. The experimental results show that the highest COP at SHX 0.90 is 0.45 with a minimum temperature of 0.93 ℃. When the SHX equals 0.85 the COP hits its highest point of 0.34, while driving temperature at 120 ℃, and the minimum temperature recorded was 0.5 ℃. So, when the SHX is 0.80 the COP hits its highest value of 0.24 when the driving temperature is 140 ℃, and the minimum temperature is 0.56 ℃ respectively. This behavior shows how more refrigerant is produced at moderate temperatures, but when the heat gets too high, the process becomes less efficient because of thermodynamic losses.

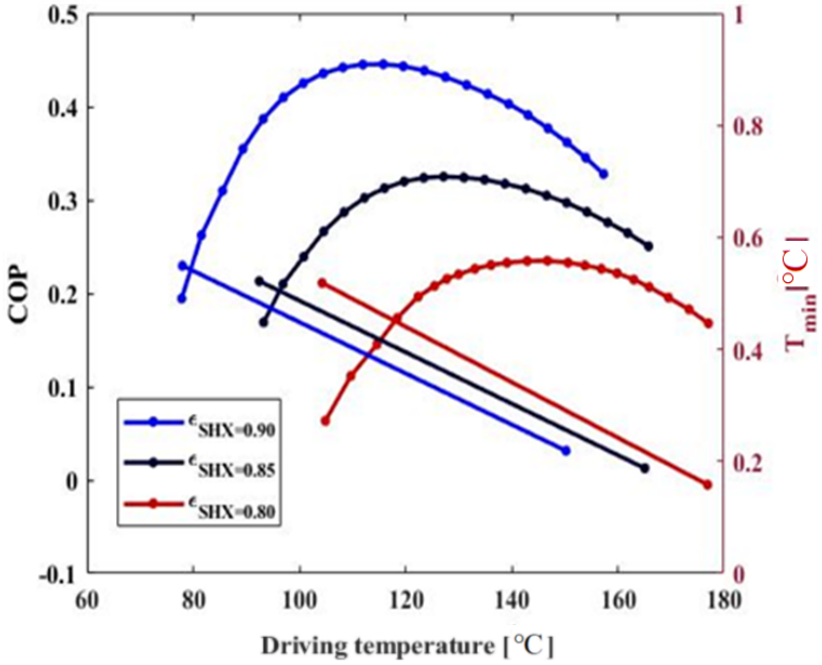

Figure 8. Coefficient of performance at different solution heat exchangers.

When the solution heat exchanger works more effectively, the COP improves because more heat is recovered internally. This means the system uses energy better and the generator doesn't need to produce as much heat. Very low T_{min} values at high driving temperatures can also create real challenges in designing heat exchangers. Overall, the results show that improving the effectiveness of the solution heat exchanger not only boosts the COP but also broadens the range of optimal operating conditions, making it important for energy-efficient design in diffusion absorption refrigeration systems.

4.7. Effect of refrigeration capacity on evaporator

Figure 9 shows how the refrigeration capacity changes with evaporator temperature under two operating conditions. Both refrigeration capacity curves show almost a straight-line pattern. As the evaporator temperature goes up from −15 ℃ to 25 ℃, the refrigeration capacity rises from 25 to 85 W. The other curve shows the evaporator temperature dropping from 25 to −18 ℃, while the refrigeration capacity goes down from around 90 to 20 W. This trend shows how much the system's refrigeration performance depends on the operating conditions of the evaporator.

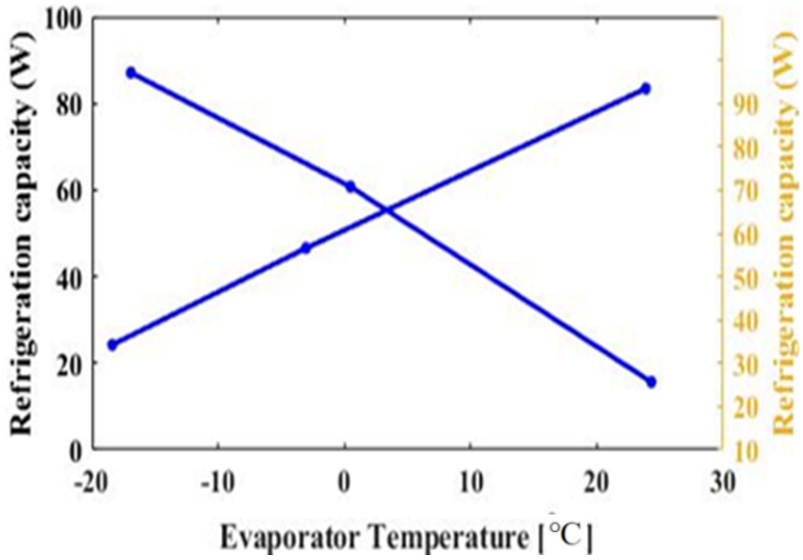

Figure 9. Performance graph for refrigeration capacity.

As the refrigeration capacity goes up, the evaporator's temperature also rises, which leads to more heat being transferred from the cooled space to the evaporator and better evaporation of the refrigerant. Higher evaporator temperatures reduce the temperature difference inside the evaporator because the heat absorption gets better, which lowers irreversibility. The second curve shows a different pattern, where increasing the evaporator temperature actually lowers the cooling effect. This might happen because of limits in how the solution circulates or the mass flow rate, which reduces the driving force needed for cooling under certain conditions. The results show that there's a specific temperature range for the evaporator where the refrigeration capacity is at its best. This makes it clear that keeping the evaporator temperature in check is really important for the system to run smoothly and efficiently.

4.8. Influence of COP and cooling power on generator temperature

Figure 10 shows the cooling capacity as a function of generator temperature and COP for different experimental conditions. The cooling capacity is the highest (121 W) at the generator temperature of 174 ℃ with 0.40 as COP. Accordingly, when the COP is 0.05, the cooling capacity could not be measured, because no refrigerant was generated in the bubble pump. Accordingly, it is considered that as the COP increases, the mass flow rate in the bubble pump increases, thereby requiring more circulation of the refrigerant. In the case of cooling power, at a generator temperature of 175 ℃, the cooling capacity generated is even at 22, and low refrigerant circulation

thereby resulting in the least vapor generation in the generator. Subsequently, when the generator temperature is 215, the cooling power is 83 W.

The cooling power shows a declining trend with increasing generator temperature. Higher cooling power values are noted at minimum generator temperatures (≈170–180 ℃), while a major reduction occurs beyond 200 ℃. This behavior may be due to increased internal losses at elevated generator temperatures and lowering effective mass flow rate, which restricts the higher refrigeration effect in spite of greater thermal input. The opposing trends of cooling power and COP emphasize that the operating at elevated generator temperatures endorses energy efficiency, while lower temperatures favor larger cooling capacity. These results underscore the requirement of careful temperature of generator optimization depending on whether cooling output or efficiency is prioritized in system design and operation.

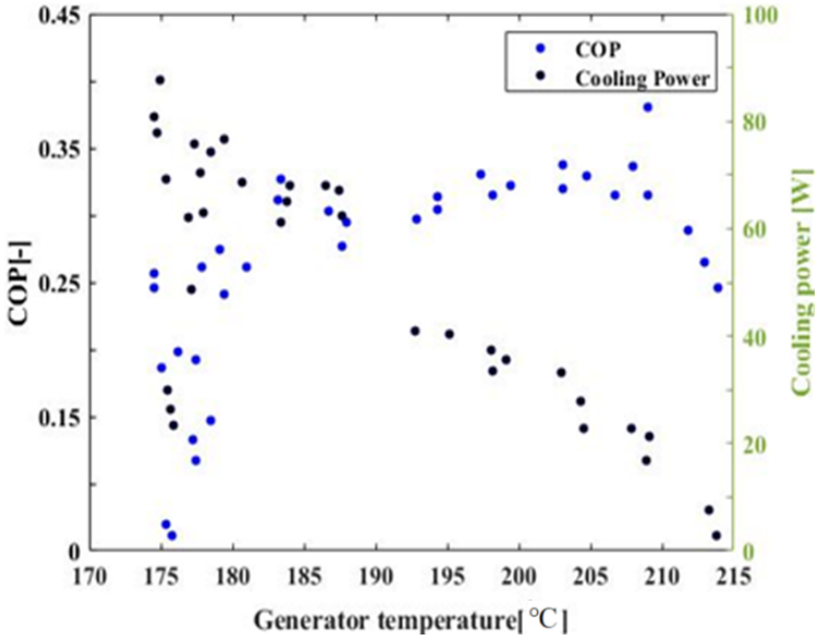

Figure 10. Performance graph for cooling power.

4.9. Performance comparison with previous studies

The performance comparison of the proposed work with previous papers is exhibited in **Table 2**. The outcome reveals that the proposed system shows the maximum COP of 0.45 which is considerably greater compared to previous research papers. For instance, Conventional working fluids exhibit maximum COP of 0.298 reported by Zohar et al. [16], Najjaran et al. [10] reported highest COP of 0.26, conventional Ammonia–Water systems show a peak COP of 0.298, as reported by Adjibade et al. [17]. Similarly, Elsayed et al. [18], reported a COP of 0.235 for an ammonia–water–hydrogen system. Gawon Lee et al. [20] reported a COP of 0.162 using R600a/n-octane/Helium working fluid in their research. Cuma Çetiner [23] reported a COP of 0.398 using $NH_3/H_2O/H_2$ working fluid. Peak COP reported by Garma et al. [24] is 0.175 followed by Harraz et al. [26] was 0.33 using organic working fluids. Mustafa Ali Ersöz [29] reported a COP of 0.36 using ammonia–water–hydrogen DAR system.

Table 2. Performance comparison of previous papers.

Authors	Working fluid	COP
Zohar et al. [16]	R124/R32/R125/R134/NH_3/H_2O	0.298
Najjaran et al. [10]	NH_3/H_2O/H_2	0.26
Adjibade et al. [17]	NH_3/H_2O/H_2	0.298
Elsayed et al. [18]	NH_3/H_2O/H_2	0.235
Lee et al. [20]	R600a/n-octane/He	0.162
Çetiner [23]	NH_3/H_2O/H_2	0.398
Garma et al. [24]	R600a-n-nonane-He	0.175
Harraz et al. [26]	Organic working fluids	0.33
Ersöz [29]	NH_3/H_2O/H_2	0.36
Proposed	R600a/DMF/He	0.45

Past studies reveal that the maximum COP of 0.36 reported by Mustafa Ali Ersöz [29], prior to the proposed work. Despite the fact that the proposed system surpasses this value by a substantial margin, indicating an enhancement approximately 25%. The improvement of performance may be due to the better thermodynamic properties of the isobutane–dimethylformamide–helium working fluid blend, comprising lower system irreversibilities, improved heat transfer characteristics and better refrigerant–absorbent compatibility. Overall, the comparison confirms that the chosen working fluid blend greatly enhances system efficiency, representing its strong potential for better performance in diffusion absorption refrigeration systems.

5. Conclusion

This study demonstrated a thermodynamic analysis of the diffusion absorption refrigeration (DAR) system by observing the impact of operating pressure, evaporator temperature, driving temperature, circulation ratio, effectiveness of solution heat exchanger and solution concentrations. The results show that the maximum coefficient of performance (COP) of 0.45 exhibits at the operating pressure 400 kPa at driving temperature of 100 ℃. Increasing the driving temperature leads to reduction in COP due to limitations in heat and mass transfer processes, greater circulation ratio and higher internal irreversibilities.

The analysis of solution concentration results that both weak and strong solution concentrations decrease by lowering the increase of driving temperature, confirming improved separation of refrigerant at moderate generator temperatures. In addition, lowering the mass flow rate with the increase in driving temperature, at higher circulation ratio, emphasizes the coupled thermal–hydraulic behavior governing DAR system operation. The effectiveness of the solution heat exchanger has an important role in performance improvement, with better effectiveness greatly enhancing COP and decreasing internal temperature mismatches. Further, the refrigeration capacity analysis represents a greater dependence on evaporator temperature, emphasizing the significance of evaporator operating conditions for stable and efficient refrigeration.

The proposed working fluid blend (R600a-DMF-He) performs maximum COP of 0.45 which is higher compared to the previously reported literature. Overall, the outcomes underscores the importance of operating pressure, internal heat recovery

mechanisms and optimizing driving temperature for attaining high performance DAR system. The proposed system shows strong potential for renewable energy-driven and low-grade heat refrigeration applications.

Author contributions: Writing—original draft, SV; writing—review and editing, GT. Both authors contributed equally to the conception, design, data collection, analysis and writing of this study. Both authors have read and agreed to the published version of the manuscript.

Funding: This work received no external funding.

Institutional review board statement: Not applicable.

Informed consent statement: Not applicable.

Data availability statement: Data sharing is not applicable to this article.

Conflict of interest: The authors declare no conflict of interest.

References

1. Pavanello F, De Cian E, Davide M, et al. Air-conditioning and the adaptation cooling deficit in emerging economies. Nature Communications. 2021; 12(1): 6460. doi: 10.1038/s41467-021-26592-2
2. Wang H, Zhao L, Cao R, et al. Refrigerant alternative and optimization under the constraint of the greenhouse gas emissions reduction target. Journal of Cleaner Production. 2021; 296: 126580. doi: 10.1016/j.jclepro.2021.126580
3. Bolaji BO. Theoretical assessment of new low global warming potential refrigerant mixtures as eco-friendly alternatives in domestic refrigeration systems. Scientific African. 2020; 10: e00632. doi: 10.1016/j.sciaf.2020.e00632
4. Khelifa S, Ramadan K, Ammar MAH, et al. Performance evaluation of an absorption refrigeration system using R1234yf-organic absorbents working fluids. Science and Technology for the Built Environment. 2021; 27(7): 936–947. doi: 10.1080/23744731.2021.1913380
5. Lima AAS, Leite GdNP, Ochoa AAV, et al. Absorption refrigeration systems based on ammonia as refrigerant using different absorbents: Review and applications. Energies. 2020; 14(1): 48. doi: 10.3390/en14010048
6. Al-Falahi A, Alobaid F, Epple B. Thermo-economic comparisons of environmentally friendly solar assisted absorption air conditioning systems. Applied Sciences. 2021; 11(5): 2442. doi: 10.3390/app11052442
7. Abedin R, Shen Y, Flake JC, et al. Deep eutectic solvents mixed with fluorinated refrigerants for absorption refrigeration: A molecular simulation study. The Journal of Physical Chemistry B. 2020; 124(22): 4536–4550. doi: 10.1021/acs.jpcb.0c01860
8. Gardenghi ÁR, Lacerda JF, Tibiriçá CB, et al. Numerical and experimental study of the transient behavior of a domestic vapour compression refrigeration system—Influence of refrigerant charge and ambient temperature. Applied Thermal Engineering. 2021; 190: 116728. doi: 10.1016/j.applthermaleng.2021.116728
9. Kong D, Yin X, Ding X, et al. Global optimization of a vapour compression refrigeration system with a self-adaptive differential evolution algorithm. Applied Thermal Engineering. 2021; 197: 117427. doi: 10.1016/j.applthermaleng.2021.117427
10. Najjaran A, Freeman J, Ramos A, et al. Experimental investigation of an ammonia-water-hydrogen diffusion absorption refrigerator. Applied Energy. 2019; 256: 113899. doi: 10.1016/j.apenergy.2019.113899
11. Srikhirin P, Aphornratana S. Investigation of a diffusion absorption refrigerator. Applied Thermal Engineering. 2002; 22(11): 1181–1193. doi: 10.1016/S1359-4311(02)00049-2
12. Zhang B, Chen W, Sun Q, et al. Numerical Evaluation of Thermal Performances of Diffusion–Absorption Refrigeration Using 1,3-Dimethylimidazolylium Dimethylphosphate/Methanol/Helium as Working Fluid. Energy Conversion and Management. 2017; 152: 201–213. doi: 10.1016/j.enconman.2017.09.048
13. Gurevich B, Zohar A. Analytical model for the prediction of performance of a solar driven diffusion absorption cooling system. International Journal of Thermodynamics. 2021; 24(4): 42–48. doi: 10.5541/ijot.929863

14. Wankhede SV, Hole JA, Patil BL. Performance of tetrafluoroethane (R134a)-dimethyl formamide diffusion absorption air cooling system with variable power input. International Journal of Ambient Energy. 2020; 43(1): 2019–2025. doi: 10.1080/01430750.2020.1722225
15. Wang Q, Liu YL, Wang SK, et al. Experiments on the performance of bubble pumps with R134a/R23-DMF solutions for diffusion absorption refrigerator. Applied Thermal Engineering. 2020; 177: 115481. doi: 10.1016/j.applthermaleng.2020.115481
16. Zohar A, Jelinek M, Levy A, et al. Performance of diffusion absorption refrigeration cycle with organic working fluids. International Journal of Refrigeration. 2009; 32(6): 1241–1246. doi: 10.1016/j.ijrefrig.2009.01.010
17. Adjibade MIS, Thiam A, Awanto C, et al. Dynamic investigation of the diffusion absorption refrigeration system NH_3-H_2O-H_2. Case Studies in Thermal Engineering. 2017; 10: 468–474. doi: 10.1016/j.csite.2017.10.006
18. Elsayed M, Attia A, Tawfeek S. Steady state numerical simulation and studying performance of a modified diffusion absorption refrigeration cycle. Alexandria Engineering Journal. 2022; 61(4): 2591–2600. doi: 10.1016/j.aej.2021.07.027
19. Valiyandi S, Thampi G. Forecasting the performance of a diffusion absorption refrigeration system using optimal fluid blend—A neural network approach. Environmental Progress & Sustainable Energy. 2022; 41: e13890. doi: 10.1002/ep.13890
20. Lee G, Choi HW, Kang YT. Cycle performance analysis and experimental validation of a novel diffusion absorption refrigeration system using R600a/n-octane. Energy. 2021; 217: 119328. doi: 10.1016/j.energy.2020.119328
21. Sözen A, Keçebaş A, Gürbüz EY. Enhancing the thermal performance of diffusion absorption refrigeration system by using magnesium aluminate spinel oxide compound nanoparticles: An experimental investigation. Heat and Mass Transfer. 2021; 57: 1583–1592. doi: 10.1007/s00231-021-03046-5
22. Senthilkumar A, Anderson A, Sekar M. Performance analysis of R600a vapour compression refrigeration system using CuO/Al_2O_3 hybrid nano lubricants. Applied Nanoscience. 2021; 13: 899–915. doi: 10.1007/s13204-021-01936-y
23. Çetiner C. Thermal analysis of operating a solar-powered diffusion absorption refrigerator with a parabolic collector. Case Studies in Thermal Engineering. 2024; 53: 103893. doi: 10.1016/j.csite.2023.103893
24. Garma R, Ben-Ezzine N, Bellagi A. Experimental and numerical investigation on diffusion-absorption refrigeration system using low GWP refrigerant R600, C_9H_{20} and helium. International Journal of Thermofluids. 2025; 27: 101246. doi: 10.1016/j.ijft.2025.101246
25. Valiyandi S, Thampi G. Solution concentration influence on the performance of a diffusion absorption refrigeration system using different refrigerant blend. Journal of Scientific Research. 2025; 17(2): 457–470. doi: 10.3329/jsr.v17i2.75859
26. Harraz AA, Haslam AJ, Mac Dowell N, et al. Computer-aided molecular design of diffusion–absorption refrigeration modules for low-temperature solar collectors. Energy Conversion and Management. 2025; 343: 120067. doi: 10.1016/j.enconman.2025.120067
27. Gurevich B. Performance analysis of diffusion–absorption refrigerator operating with MgAl2O4 nanoparticles and R1234yf–DMAC. International Journal of Refrigeration. 2026; 185: 54–61. doi: 10.1016/j.ijrefrig.2026.02.009
28. Zebbar S, Zebbar D, Rahmani Z. CFD analysis of an evaporator in diffusion absorption refrigeration systems using helium as an auxiliary gas. International Journal of Refrigeration. 2026; 183: 95–107. doi: 10.1016/j.ijrefrig.2026.01.003
29. Ersöz MA. Investigation the effects of different heat inputs supplied to the generator on the energy performance in diffusion absorption refrigeration systems. International Journal of Refrigeration. 2015; 54: 10–21. doi: 10.1016/j.ijrefrig.2015.02.013